Diamond-based Radiation Sensor for LENR Experiments. Part 1: Sensor Development and Characterization

Eric Lukosi,* Mark Prelas, Joongmoo Shim, Haruetai Kasiwattanawut, Charles Weaver, Cherian Joseph Mathai and Shubhra Gangopadhyay

SKINR, University of Missouri, Columbia, MO 65211, USA

Abstract

There have been many reports on charged particle and neutron production in LENR experiments but as of yet they have not been correlated in time with excess heat generation. Diamond sensors with palladium electrodes can be utilized to address this need. First results using a diamond sensor are presented.
© 2014 ISCMNS. All rights reserved. ISSN 2227-3123

Keywords: Charged particle spectroscopy, Diamond sensors, Low energy nuclear reactions

1. Introduction

LENR experiments are done in three basic ways: gas loading, plasma loading/co-deposition, and electrochemically. If radiation is a by-product of LENR then their detection is limited by a few basic factors. In the case of neutrons the detection efficiency of the sensor for the source of interest must be statistically higher than background. For charged particles, the system must also be designed to keep background noise and count levels as low as possible. In addition, the distance between the detector and the charge particle emitting source should be minimized to limit energy loss outside of the sensing medium. This is especially important if spectroscopic analysis is going to be conducted.

Experimental analyses of charged particle and neutron production in LENR have utilized CR-39. At first the sensors were placed near electrodes in electrochemical cells and later were placed in direct contact. Results of this work indicate that there seems to be charged particle production by single track analysis using unfolding software, but later experiments placed the sensor in direct contact with the electrode [1–4]. Neutron production was also considered a possibility at a minimum energy of 7.89 MeV due to triple tracks produced by three alpha particles from the breakup of ^{12}C [1,2,5].

There are many limitations in using CR39 for radiation detection as outlined by Durrani in 2008 [6]. In this application the major limitation is the limited spectroscopic capabilities of CR39. To understand better, the mechanism

---
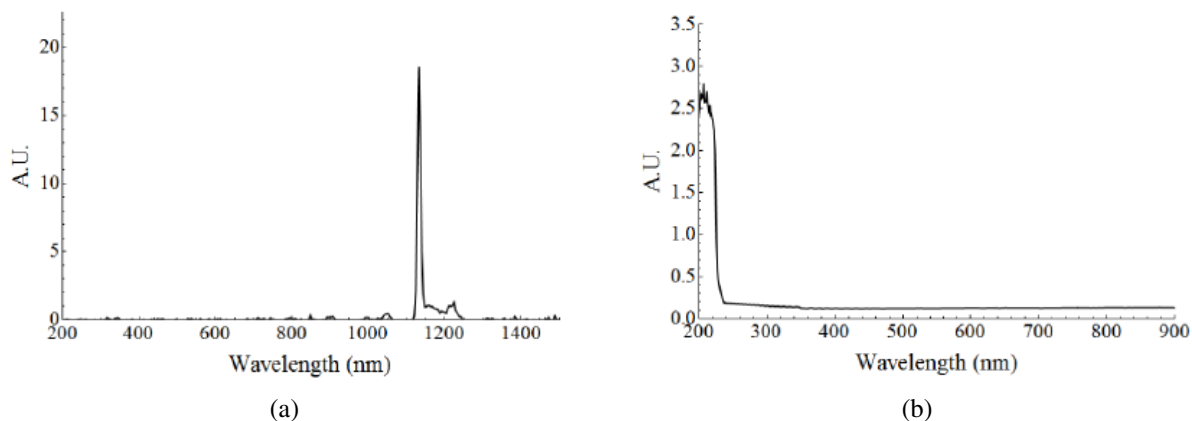
*E-mail: edlf3f@mail.missouri.edu

Figure 1. Count rate data for the hydrogen exposures of the palladium coated sensor for (a) the entirety of the experiment and (b) during the count rate burst.

of LENR it is vital to conduct spectroscopy on the created charged particles and/or neutrons in an LENR experiment and to correlate them in time with excess heat generation in order to provide definitive evidence whether or not the two are correlated. If they are correlated, conducting an analysis of the change in energy due to the supposed nuclear reaction would be a great step in understanding the reaction mechanism(s) of LENR reported by so many in recent history.

2. Diamond Sensor Background

To begin to answer the identified need, it is proposed that diamond be used for radiation detection in LENR experiments. Diamond is a wide band gap semiconducting material that is radiation hard, mechanically the strongest material known to man, chemically inert, and exhibits an extremely high thermal conductivity [7]. These properties allow a diamond sensor to be used in a variety of environments and operated at various temperatures. Diamond can act as a radiation sensor because of its semiconducting properties and the commercial availability of intrinsic grade single crystal diamond plates. This makes diamond suitable for both charged particle and neutron detection.

    Charged particles and photons can be detected by diamond through the collection of electron–hole pairs created within its band structure as any charged particle slows down within it. The statistically averaged ratio of electron–hole pairs created versus total energy deposition is 0.42 for diamond. There have been several reports on the interactions of charged particles or photons with diamond in recent history as the capabilities of synthetic diamond growth have allowed for electronic grade diamond to become available [8–14]. This work has shown that energy resolutions for alpha particle interactions approach 0.6% [13,15] and 4% for 14.1 MeV neutrons through reaction number 8 in Table 1 [14,16]. This table indicates all the neutron–carbon interactions that can take place in a center of mass energy range from 0–20 MeV. Since diamond is a low-Z material gamma rays are not readily detectable in small diamond plates for low to moderate energies in low flux environments operating in pulse mode.

    The capabilities of diamond outlined indicate that diamond could be very suitable as a radiation sensor to replace CR39 in LENR studies. It is also excellent compared to other solid-state or gas sensors because it is wide band-gap, corrosion and radiation resistant and made with low atomic mass atoms. Among its capabilities are low thermal noise at room temperature (does not need cooling) high sensitivity (has an excellent signal to noise ratio), and is able to detect multiple types of radiation in the same sensor including charged particles and neutrons (recoil detection). However,

Table 1. Neutron interactions with natural carbon[1].

Reaction number	Reaction	Q-value (MeV)	Threshold energy (MeV)
1	$^{12}C(n,\gamma)^{13}C$	4.946	0
2	$^{12}C(n,el)^{12}C$	0	0
3	$^{12}C(n,n')^{12}C^{*}$	–	4.450[2]
4	$^{12}C(n,n')^{12}C^{*}(3\alpha)$	−7.275	7.886
5	$^{12}C(n,n')^{12}C^{*}(3\alpha)$	–	9.64[2]
6	$^{12}C(n,n')^{12}C^{*}(3\alpha)$	–	10.8[2]
7	$^{12}C(n,n')^{12}C^{*}(3\alpha)$	–	11.8[2]
8	$^{12}C(n,\alpha_o)^{9}Be$	−5.701	6.181
9	$^{12}C(n,\alpha_1)^{9}Be^{*}$	−7.381	8.800
10	$^{12}C(n,p)^{12}B$	−12.59	13.64
11	$^{12}C(n,d)^{11}B$	−13.73	14.89
12	$^{12}C(n,np)^{11}B$	−15.96	17.30
13	$^{13}C(n,\gamma)^{14}C$	8.176	0
14	$^{13}C(n,el)^{13}C$	0	0
15	$^{13}C(n,\alpha)^{10}Be$	−3.835	4.132
16	$^{13}C(n,n\alpha)^{9}Be$	−10.65	11.47
17	$^{13}C(n,t)^{11}Be$	−12.42	13.39
18	$^{13}C(n,p)^{13}B$	−12.66	13.64
19	$^{13}C(n,d)^{12}B$	−15.31	16.50
20	$^{13}C(n,np)^{12}B$	−17.53	18.89

[1]All data, unless otherwise specified, were obtained from the National Nuclear Data Center maintained by
    Brookhaven National Laboratory [17].
[2]Data reported obtained from Pillon et al. reported in 1995 [18].

electrochemical cells are not the best environment to obtain better information about charged particle energy in the
current design because of the loss of energy in the fluid which separates the sensor from the deuterium loaded film and
the various path lengths that charged particles can take. This is also a problem in the gas loading LENR experiments
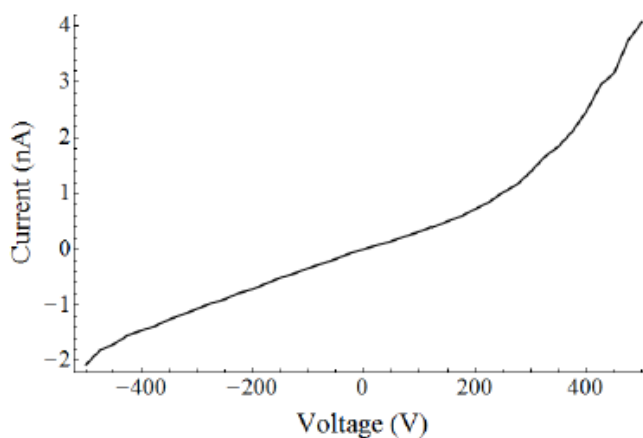

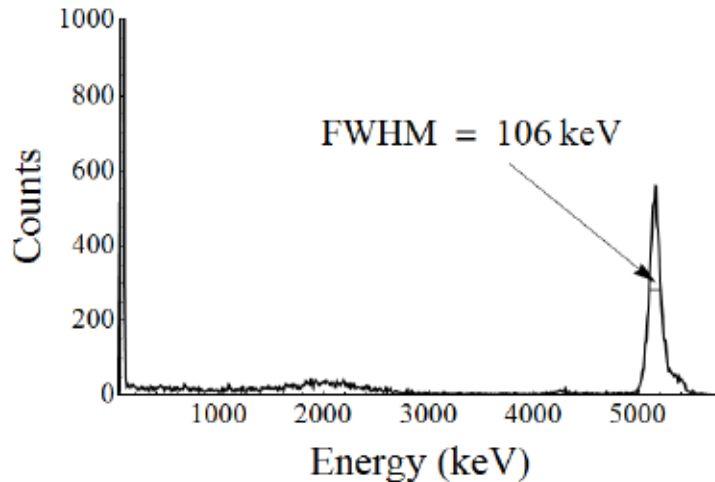**Figure 2.** $I − V$ characteristics of the diamond sensor.

Figure 3.   Pu-239 spectrum obtained with the diamond sensor.

as well and can only be overcome by operating in a vacuum for current experimental techniques.

To get past this difficulty a palladium film will be used as an electrode on the diamond sensor so that the detection efficiency of any charged particles coming from the system will be 0.5 and is also the geometrical detection efficiency of any neutrons coming from the palladium film. In this configuration the energy lost by the charged particles will be minimized and well controlled, occurring only within the thin (100 nm) palladium film. In this manner diamond can be utilized in both gas loaded and electrochemical experiments. In the former the detector is merely introduced to a high pressurized deuterium environment and in the latter one of the diamond electrodes can be utilized as an electrode such that it creates a parallel component to the electrochemical cell. The high resistance of diamond makes current flow into
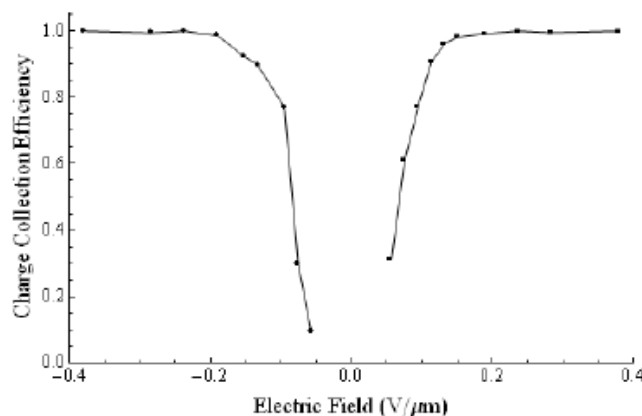

Figure 4.   Charge collection efficiency versus applied bias across the diamond sensor during Pu-239 exposures.
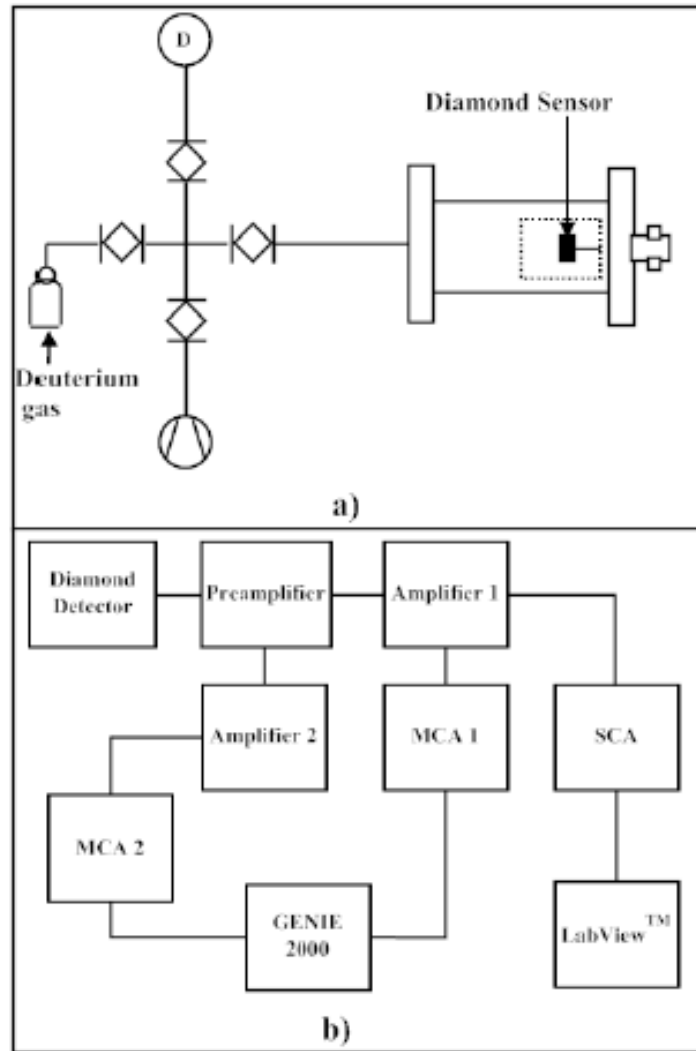
Figure 5. In (a) the experimental setup is described and the electronic pathways are shown in (b).

the detection system very low unless a radiation interaction occurs in which case one type of charge carrier (electrons or holes) will be collected by the detection system.
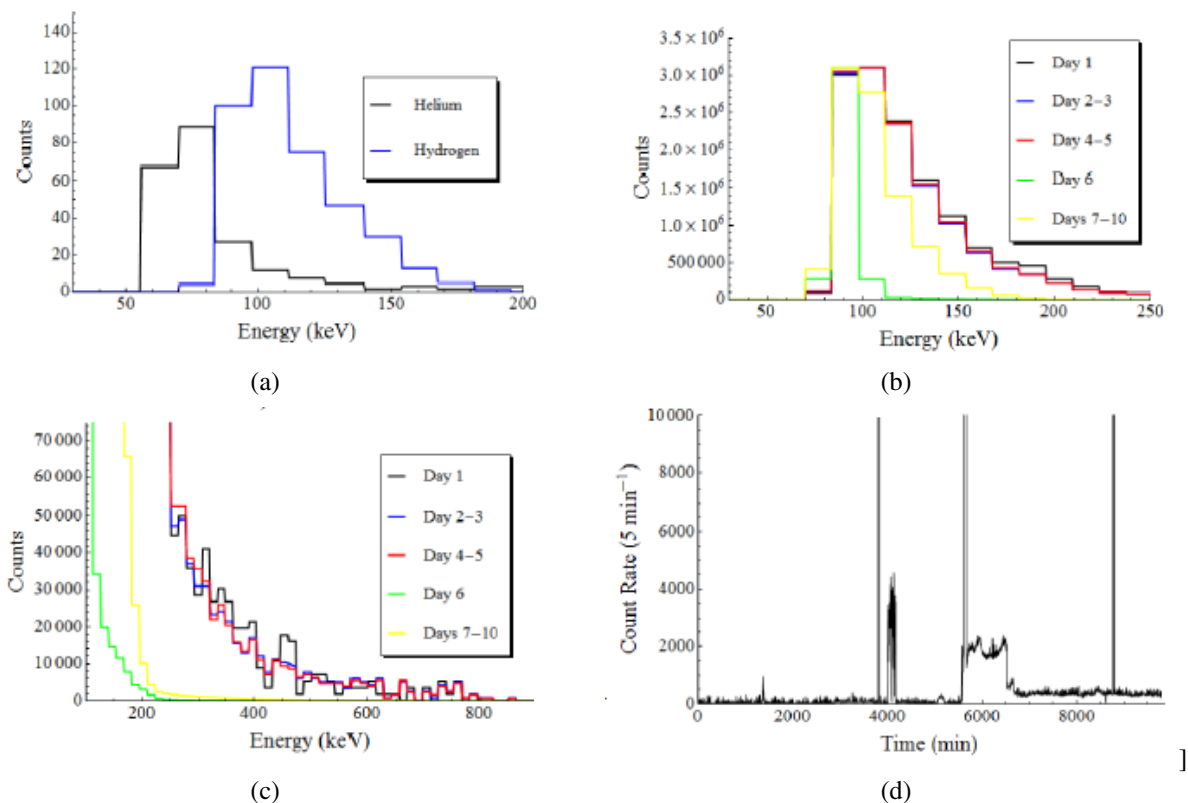
Figure 6. Experimental results obtained in the gas loading palladium electrode on a diamond sensor. Here the results are shown for (a) the background spectra obtained for hydrogen and helium, (b) and (c) the low-energy spectra from the deuterium run, and (d) the count rate of pulses observed in the diamond sensor over time for the deuterium run.

3. Experimental Technique

3.1. Sensor material

Two $3 \times 3 \times 0.5$ mm semiconducting diamond plates were obtained from Element Six for this work [19]. The diamonds were characterized through Raman and spectrophotometry to verify its structure and detect any band gap impurities. The results shown in Fig. 1 indicate that the samples have no energy levels within the band gap that are above the detection threshold for the spectrophotometer used.

　　The diamond samples were chemically cleaned with the following process and were rinsed with deionized water between each step. The first two steps are meant to clean the diamonds and remove any stray metal and organic materials. The last two steps are utilized to remove any graphitization layers on the surface and to oxygen terminate the surface to increase the surface resistivity of the diamond.

(1) Aqua Regia at 150°C for 20 min.
(2) $NH_3OH/H_2O_2/H_2O$ (1:1:5) at 150°C for 20 min.
(3) Piranha at 150°C for 20 min.
(4) $H_2SO_4/HNO_3/HClO_4$ (1:1:1) at 150°C for 30 min.

The diamonds were metalized through sputtering carbon at 400°C to create an approximate 10 nm diamond-like carbon (DLC) layer and then coated with a palladium top layer 100 nm thick. The DLC layer provides two functions. First, it provides a junction between the electrode and diamond for mechanical adhesion. Second, it provides a tunneling junction for electrons to escape the diamond material when a large work function metal is used as the electrode [13]. This allows for the creation of a contact that should behave Ohmically.

3.2. Sensor electrical characterization

The diamond was mounted on a transistor head and wire bonded with aluminum. Its current–voltage properties were characterized using a Keithley 6487 picoameter and the results are shown in Fig. 2. It can be seen that the sensor does behave Ohmically for lower voltages but that a somewhat Schottky behavior is observed at voltages above +250 V. This was found to be due to the conductive silver epoxy on the diamond outside of the palladium contact area and was verified by reversing the circuit configuration for this measurement and seeing the same effect with an opposite applied voltage. In any case, it is shown in the following alpha particle exposures that a bias of 200 V is all that is required to gain 100% charge collection efficiency and so the observed Schottky behavior is unimportant.

The diamond sensor was then tested for its energy resolution and charge carrier characteristics through the use of a Pu-239 alpha source and Hecht's theory (Eq. (1)), which relates the charge collection efficiency to the properties of the semiconductor. It can then be used to characterize the mobility-trapping time constant product of the sensor (Eq. (2)) and therefore the required bias to collect 100% of the charge generated. The energy resolution of the diamond sensor used is pictorially shown in Fig. 3 to be 2.1%.

By exposing the diamond to alpha particles and varying the applied bias used for charge collection a plot can be created that relates the charge collection efficiency to the applied electric field. The diamond sensor was utilized with an Ortec 142PC preamplifier, Canberra 2026 spectroscopy amplifier, and Genie 2000 for data acquisition. A plot of these results is given in Fig. 4.

$$Q_{\mathrm{c}} = Q_0 \left[\frac{\mu_{\mathrm{e}} \tau_{\mathrm{e}} E}{W} \left(1 - \mathrm{e}^{-x/\mu_{\mathrm{e}} \tau_{\mathrm{e}} E} \right) + \frac{\mu_{\mathrm{h}} \tau_{\mathrm{h}} E}{W} \left(1 - \mathrm{e}^{-(W-x)/\mu_{\mathrm{h}} \tau_{\mathrm{h}} E} \right) \right], \tag{1}$$

$$\frac{\mu_{\mathrm{e}}}{h} \frac{\tau_{\mathrm{e}}}{h} = \frac{W}{E}. \tag{2}$$

The result of the alpha particle exposures yielded the data shown in Table 2. These exposures also allowed the characterization of the energy resolution of the diamond sensor, which was 2.43 and 2.37% for a positive and negative applied bias, respectively. The sensor did not exhibit polarization effects at a positive bias of 200 V over a one-hour exposure. Further, it has been shown experimentally that diamond responds linearly with deposited energy and agrees with theory such that the location of the Pu-239 alpha particle peak can be used for a one-point energy calibration [20]. The location of the Pu-239 peak in the pulse height spectrum was determined for various amplification factors and it was found to be linear, as expected.

3.3. Experimental setup and procedure

A schematic of the experimental apparatus and the electronic acquisition system setup for the deuterium gas loading experiment are shown in Fig. 3. In (a) the experimental set-up is shown where the diamond is placed inside of a small pressure vessel that can handle up to 690 kPa. The voltage applied to the sensor was +200 V during all experimental runs where the top electrode carries the positive potential with respect to ground. Here, the signal from the preamplifier was

Table 2. Charge carrier characteristics of the diamond sensor.

	Electrons	Holes
Median $\mu\tau$ (10^{-6}cm^2/V)	59.3	67.6
Maximum $\mu\tau$ (10^{-6}cm^2/V)	60.4	71.1
Minimum $\mu\tau$ (10^{-6}cm^2/V)	58.2	64.8

split and sent to two different amplifiers. This allowed for simultaneous measurement of fine low-energy spectroscopy as well as very high-energy spectroscopy. The high-energy and low-energy signals are denoted as Amplifiers 1 and 2 with full scales of 59 and 5.7 MeV, respectively. The low-energy spectrometer had its signal split from its output to go to both the MCA and an SCA and then to a digital counter that allows for some timing information on the pulses. Although this method does not allow each pulse to be time-stamped, it does allow the quantification of rapid increases of count rates during experiments as it has been indicated in several LENR experiments that excess heat generation often takes place in pulses.

The experimental procedure started with loading the diamond sensor into the test chamber and the chamber was evacuated using a mechanical pump to approximately 1 mTorr. The chamber was then filled with the process gas to a pressure of approximately 5100 Torr and placed into a lead shield three inches thick above the chamber and one and a half inches thick else. Three gases were utilized in this experiment: helium, hydrogen, and deuterium. The first process gas was used to determine the background counts that can be expected and was conducted for 1 h. Then natural isotopic abundance hydrogen was used as a check for a secondary background count experiment. Then the system was evacuated to 1 mTorr for 3 h to unload any light hydrogen from the electrode and the final run using deuterium was conducted. The pressure used in the gas loading is expected to lead to a D/Pd loading ratio of approximately 75%. This was not verified during the experiment but can be a future addition to the system through resistance measurements of the top electrode.

4. Results

The spectra obtained in this experiment are shown in Fig. 6. The background spectra for helium and hydrogen, taken for one hour each, are shown together in part (a). The background spectra for each of the process gases give the general shape. The Ortec 142PC preamplifier has a sensitivity with diamond at its input of 80 mV/MeV and for the helium run this indicates that the peak of the noise lies around 16 mV. For the hydrogen run the noise shifted by a channel number and so the noise floor of the MCA had to be shifted by one channel to keep the dead time down and is the reason for the difference between the spectra.

The deuterium run spectra are shown in parts (b) and (c). Spectra were taken at various times in this experiment to provide a measure of spectral change over time. The spectra obtained were normalized to each other and the ratio of the run time and maximum count in a channel to the largest count rate spectrum is given in Table 3. This data clearly indicates that the count rate seen is not constant over the ten-day run.

In part (b) the low-energy spectrum obtained for the deuterium gas loading experiment is shown. It can be seen that the run using deuterium process gas differs from the background runs by a tail of pulses that extends into higher energies. This can be seen clearly in part (c) that shows a low total count scale on the ordinate. The energy of the pulses seen are distributed and do not match what is expected for a nuclear reaction, such as a narrow peak from alpha decay. Further, the data obtained for day six clearly shows a massive jump in counts versus the other spectra obtained at the

Table 3. Normalized time and count data of all experimental data obtained for the pressurized deuterium runs.

Run	Day 1	Days 2–3	Days 4–5	Day 6	Days 7–10
Time	4.24	2.15	1.96	5.00	1.00
Counts	1788.2	861.3	787.7	17.8	1.00

location of the peak of all spectra shown. The actual peak of this spectrum was 209,775 counts at channel number 6, corresponding to 80 keV.

Only one spectrum was obtained after day six and it was conducted for 3 days. There is an interesting effect in this spectrum in that the location of the peak is now pushed against the lowest channels, as if it has been shifted to lower energies even though there is no cause for this shift due to equipment changes or faults and was verified with other sensors. The high-energy spectra are not shown here because no high energy counts were registered in any of the experimental runs at any time.

To compare the obtained spectra, the rate of counts registered per 5 min period from day three and on is displayed in part (d). It can be clearly seen that the count rate is very low for about the first 3800 min and at about this time the count rate increases rapidly for a short period. This occurs a second time shortly after at about 4000 min with a large width and then a third time at about 4600 min with a very long high count rate plateau ending at about 6600 min. There is also a final fourth count rate burst as well at about 8700 min and after the third count rate burst the background count level floor is increased by about a factor of two. This seems to indicate that there are possible spontaneous reactions of some kind depositing energy (or more accurately charge in the conduction band of the diamond or into the high input of the preamplifier) within the diamond sensor. It is possible that the burst in count rate is some sort of electronic noise and further analysis is required in future experiments. However, all electronics associated with these measurements were plugged into a power conditioner and so this seems unlikely.

A visual representation of the electrode before and after the experiment is shown in Fig. 7. After inspection it becomes clear that some sort of reaction has indeed occurred between the diamond sensor electrode and the deuterium gas. At this point it is unclear whether the damage to the electrode is chemical or nuclear in nature.

It is not expected to be directly due to the potential on the electrode, although there may be some indirect effects of having a positively charged electrode in a pressurized deuterium atmosphere. It is possible that the effect of a higher background count rate between the third and fourth count rate bursts could be due to vibrational effects on a partially delaminated palladium electrode. The sensor was tested for operability after the deuterium run was halted and it responded as expected to a Pu-239 alpha particle source. However, when another background run in hydrogen was tried the palladium top electrode was lost during chamber evacuation and/or pressurization.

5. Conclusion

In this work the preparation and application of a diamond sensor to a gas loading palladium LENR experiment has been presented. The results obtained indicate that some sort of reaction has taken place when the sensor was in the deuterium environment due to electrode deformation and delamination and due to the different pulse height spectra seen between runs conducted in hydrogen and deuterium. Further analysis of the observed effects is required. In part two of this report the diamond sensor will be exposed to a pressurized hydrogen environment for several days to see if the observables are due to chemical reactions with the palladium electrode. A better experimental procedure will be conducted and second run results will be presented.

References

[1] P.A. Mosier-Boss et al., Characterization of tracks in CR-39 detectors obtained as a result of Pd/D Co-deposition, *Euro. Phys. J. Appl. Phys*. **46** (2009) 1–12.
[2] P.A. Mosier-Boss et al., Use of CR-39 in Pd/D co-deposition experiments, *Euro. Phys. J. Appl. Phys*. **40** (2007) 293–303.
[3] A.G. Lipson et al., In-situ charged particles and X-ray detection in Pd thin film-cathodes during electrolysis in Li_2SO_4/H_2O, in *Ninth Int. Conf. on Cold Fusion,* 2002, Beijing, China.
[4] R.A. Oriani and J.C. Fisher, Generation of nuclear tracks during electrolysis, *Japanese J. Appl. Phys.* **41** (2002) 6180–6183.
[5] P.A. Mosier-Boss et al., Comparison of Pd/D co-deposition and DT neutron generated triple tracks observed in CR-39 detectors, *Euro. Phys. J. Appl. Phys*. **51** (2010) 1–10.
[6] S.A. Murrari, Nuclear tracks today: Strengths, weaknesses, challenges, *Radiation Measurements* **43** (2008) S26–S33.
[7] R.S. Balmer et al., *J. Phys: Cond. Matter* **21** (2009) 364221.
[8] J. Isberg et al., *Science* **297**(5587) (2002) 1670–1672.
[9] J. Isberg et al., *Diamond and Related Materials* **13** (2004) 872–875.
[10] M. Pomorski et al., Charge carrier transport properties of single crystal CVD-diamond particle detectors, *Diamond and Related Materials* **16** (2007) 1066–1069.
[11] E. Pace, R.D. Benedetto and S. Scuderi, Fast stable visible-blind and highly sensitive CVD diamond UV photodetectors for laboratory and space applications, *Diamond and Related Materials* **9** (2000) 987–993.
[12] R.D. Benedetto et al., Influence of metal–diamond interfaces on the response of UV photoconductors, *Diamond and Related Materials* **10** (2001) 698–705.
[13] A. Galbiati et al., *IEEE Trans. Nucl*. Sci. **56**(4) (2009) 1863–1874.
[14] M. Pillon et al., Radiation tolerance of a high quality synthetic single crystal chemical vapor deposition diamond detector irradiated by 14.8 MeV neutrons, *J. Appl. Phys.* **104** (2008) 054513.
[15] A. Murari et al., Measuring the radiation field and radiation hard detectors at JET: Recent developments, *Nucl. Instr. Methods in Phys. Res. A* **593** (2008) 492–504.
[16] S. Almaviva et al., Thermal and fast neutron detection in chemical vapor deposition single-crystal diamond detectors, *J. Appl. Phys.* **103** (2008) 054501.
[17] National Nuclear Data Center: p. www.nndc.bnl.gov.
[18] M. Pillon, M. Angelone and A.V. Krasilnikov, 14 MeV neutron spectra measurements with 4% energy resolution using a type II a diamond detector, *Nucl. Instr. Methods in Phys. Res. B* **101** (1995) 473–483.
[19] Element Six, King's Ride Park, Ascot, UK.
[20] M. Pillon et al., *Nucl. Instr. Methods in Phys. Res. A* **640** (2011) 185–191.